

Robotic fabric flattening with wrinkle direction detection

Yulei Qiu¹, Jihong Zhu², Cosimo Della Santina¹, Michael Gienger³ and Jens Kober¹

Abstract—Deformable Object Manipulation (DOM) is an important field of research as it contributes to practical tasks such as automatic cloth handling, cable routing, surgical operation, etc. Perception is considered one of the major challenges in DOM due to the complex dynamics and high degree of freedom of deformable objects. In this paper, we develop a novel image-processing algorithm based on Gabor filters to extract useful features from cloth, and based on this, devise a strategy for cloth flattening tasks. We evaluate the overall framework experimentally, and compare it with three human operators. The results show that our algorithm can determine the direction of wrinkles on the cloth accurately in the simulation as well as the real robot experiments. Besides, the robot executing the flattening tasks using the dewrinkling strategy given by our algorithm achieves satisfying performance compared to other baseline methods. The experiment video is available on <https://sites.google.com/view/robotic-fabric-flattening/home>

I. INTRODUCTION

Despite significant progress made in recent years, DOM is still considered one of the major challenges in robotics due to the complex dynamics and high degree of freedom of deformable objects [1], [2]. Robots should be able to manipulate them to work in a human environment, as many manipulation tasks in our daily life involve those objects, such as picking up fruits and folding clothes.

DOM tasks, like many other robotic tasks, can be broken down into perception and control. Perception in DOM is to obtain states to describe the object, while control uses this information to guide robot motion. The goal of perception and control in DOM is to efficiently infer the complex configuration of a deformable object, determine a policy for manipulation and perform an action correspondingly.

This paper concerns itself with perception and control in cloth manipulation. This challenging task has attracted much attention over the years [3]. With the development of computer vision, we are beginning to see some results in both simulations and robot experiments on how to perceive clothes. Early methods, for example, rely on extra markers [4] that require the cloth to be completely covered to infer the state, or predefined visual features [5], [6] which approximate the cloth with predefined polygon models. The use of markers is usually not possible in practical cases, and predefined geometric features are often not robust and introduce errors in state estimation [7]. Actions, policies, or strategies to

¹Department of Cognitive Robotics, Faculty of Mechanical, Maritime and Materials Engineering (3mE), Delft University of Technology, the Netherlands, yulei.qiu@outlook.com, cosimodellasantina@gmail.com, j.kober@tudelft.nl

²School of Physics, Engineering and Technology, University of York, the UK, jihong.zhu@york.ac.uk

³Honda Research Institute Europe, Germany, michael.gienger@honda-ri.de

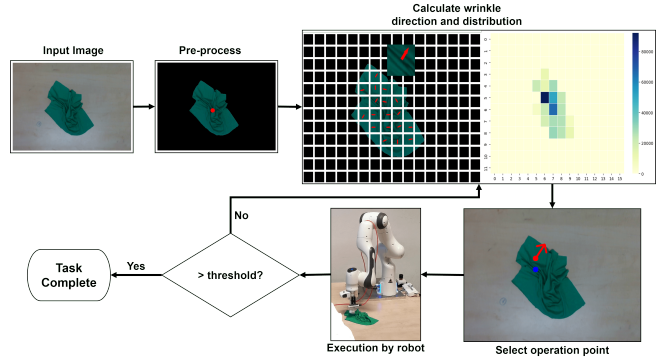


Fig. 1: Outline of the proposed cloth flattening framework

manipulate can be learned from human demonstrations since human behavior during the cloth manipulation process is difficult to model. Commonly used methods in Learning from Demonstration (LfD) include Dynamic Movement Primitives (DMPs) [8] and Gaussian Processes (GPs) [9]. Recent data-driven methods combine perception and control stages, which do not infer the explicit states of the cloth. Rather, they output the policy directly, which learn the mapping from the raw RGB(D) images to the robot actions [10]–[12]. Like most learning-based methods, they require a large amount of training data and are computationally demanding.

We developed a sensing algorithm that does not rely on markers or geometry shapes, followed by a control strategy to make use of the sensing information to do fabric flattening. They are integrated in a DOM framework for a robot to carry out cloth flattening tasks, as shown in Fig. 1. Our method calculates the magnitude and direction of wrinkles on the cloth, thereby outputs a 2D vector to represent the stretching direction which the robot can drag along to remove wrinkles, and an operation point where the robot touches the fabric. The magnitude reflects the distribution of wrinkles, which helps find the operation point. The outcomes from the perception can be directly utilized by the the robot manipulator to execute the flattening tasks.

The main contributions of this paper are:

- 1) A novel image-processing algorithm on cloth-like deformable objects that computes a stretching direction and an operation point which can be directly used by the robot manipulator.
- 2) A simple control strategy leveraging the output of the perception step to perform the flattening actions.
- 3) A framework combining the algorithm and control strategy that enables us to perform cloth flattening tasks in high efficiency compared to baseline methods.

The rest of the paper is organized as follows: Section II covers the related work. The methodology is given in Section III. The experimental validation and results are given in Section IV and V respectively. Finally, conclusions are stated in Section VI.

II. RELATED WORK

In this section, we give a brief summary of prior works on the perception and control of cloth manipulation.

Perception: Besides aforementioned perception methods [4]–[6], other work on cloth perception uses wrinkle as an intuitive visual feature [13], [14], since they are obvious when clothes are placed on a flat surfaces. These two approaches calculate a heat map from visual data, which determines the states or the grasping policies. Prior to them, a Gabor filter [15] is applied on the images to extract wrinkle features [16]. The Gabor filter with designed kernel can effectively detect the area of the cloth exhibiting wrinkles. Jia et al. [17], [18] proposed HOW features corresponding to shadow variation computed by applying Gabor filters with multiple orientations and wavelengths. We notice from the previous work that visual descriptors are possible to extract low-dimensional features of cloth-like objects from RGB-(D) data, thereby forming an effective state representation, which holds potential for utilization in other fabric manipulation tasks.

Control: Robot actions can be either determined by a controller based on the perception information (model-based) [19]–[21] or learned from the raw image input (model-free) [22], [23]. Model-based methods are generally more computationally efficient and can provide a better understanding of the underlying physics of the system, but require more prior knowledge and may not be as flexible as model-free control [24], [25]. Model-free methods like Imitation Learning (IL), demonstrate superior performance in the learning of movement policies, as they are capable of capturing the trajectory that predicts the actions of the expert given the corresponding RGB-D images [18], [26], [27]. These methods are more flexible and can be used when the dynamics of the system are not well understood, yet they require more data and can be more computationally intensive [24], [25], which is not practical in our applications.

III. METHODS

Given an input RGB image from top-down view of an cloth-like object, the algorithm can accurately identify the wrinkle direction and distribution on the cloth, thereby computing both the stretching direction and operation point. The stretching direction is perpendicular to the wrinkle, informing the direction along which the robot should apply force to remove wrinkles. The magnitude of the wrinkle indicating the distribution of the wrinkles is a key factor when determining the operation point, which is the location where the robot touches the fabric then moves along the stretching direction. Once the direction and operation point have been determined, the robot can execute the actions to flatten the cloth. After one step of action, the robot moves

up again to get a global image and run the algorithm again. The pipeline will work iteratively until the cloth is flattened.

The main components of our proposed algorithm, i.e., direction calculation and operation selection, are discussed in the following two subsections.

A. Calculate stretching direction

As previously mentioned, we have noticed that Gabor filters are effective in extracting wrinkles in images, hence are useful to infer the directions and distribution of wrinkles in an image. A 2D Gabor filter can be mathematically represented as:

$$g(x, y; \lambda, \phi, \sigma, \gamma, \theta) = \exp \left(-\frac{x'^2 + \gamma^2 y'^2}{2\sigma^2} \sin 2\pi \frac{x'}{\lambda} + \phi \right) \quad (1)$$

where $x' = x \cos \theta + y \sin \theta$, $y' = -x \sin \theta + y \cos \theta$, λ is the wavelength, ϕ is the phase offset, σ is the standard deviation of the Gaussian, γ is the spatial aspect ratio, and θ is the orientation of the normal to the parallel stripes of the Gabor filter. Fig. 2 shows that the outputs of the Gabor filter in some orientations highlight wrinkles in the corresponding directions.

Fig. 1 shows an overview of how to calculate the direction. The raw RGB image from the camera is first processed by HSV thresholding to remove the background and leave the cloth part only. The center of mass (CoM, denoted by a red dot in Fig. 1) of the cloth is computed. Besides, the image \mathbf{I} is split into N small blocks $\{\mathbf{I}_j\}, j = 0, 1, \dots, N - 1$. The algorithm that calculates the stretching direction is shown in Alg. 1. As inputs it receives those block images $\{\mathbf{I}_j\}$, CoM the number of orientations of Gabor filter n . The Gabor filter is applied in the following orientations:

$$\theta_i = i \times \frac{\pi}{n}, \forall i \in \{0, 1, \dots, n - 1\} \quad (2)$$

The magnitude l_i of the wrinkles in a particular orientation θ_i is quantified by computing the sum of values across all

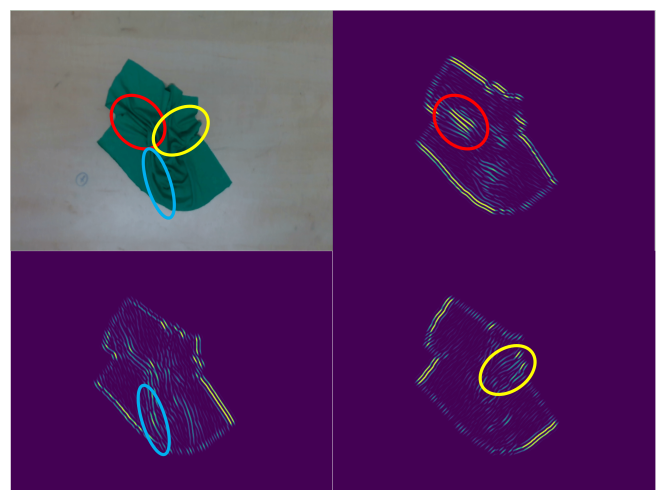


Fig. 2: Gabor filter highlights wrinkles in different orientations. Orientation $\theta = 123.75^\circ$ (Top Right), 157.5° (Bottom Left), 45° (Bottom Right)

pixels in the corresponding output map T_i of the Gabor filter:

$$l_i = \sum_{t \in T_i} t \quad (3)$$

Note that T_i can be considered as an intensity map in the given orientation θ_i (see Fig 2), and t corresponds to one value in the intensity map T_i . Therefore, the magnitude m_i of the block I_i is the highest value among all orientations $\{\theta_i\}$:

$$m = \max \{l_i\}, \forall i \in \{0, 1, \dots, n - 1\} \quad (4)$$

where n is the number of orientations. The reasoning behind this approach is that the orientation with the highest magnitude is likely to correspond to the direction with the most significant wrinkles.

Intuitively, if there is a wrinkle on a cloth and its direction is parallel to the x axis, a person will probably pull or stretch the cloth in the perpendicular direction of the wrinkle, which is the y axis, to flatten the cloth. Based on this intuition accordingly, the stretching direction employed to remove wrinkles should be perpendicular to the orientation, i.e. wrinkle direction. Meanwhile, to maximize the efficiency of wrinkle removal, the stretching direction should point outward from the CoM of the cloth. This condition can be verified by computing the dot product between the stretching direction w and the vector extending from the CoM to the current block (denoted as v_{cc}). If the dot product is not positive, the opposite direction will be selected.

After looping over all the block images, we will get a few directions $\{d_j\}, j = 0, 1, \dots, N - 1$ and operation points $\{m_j\}, j = 0, 1, \dots, N - 1$. With magnitudes we can draw a heatmap (see Fig. 1) showing the distribution of the wrinkles across the blocks. It is important to note that the magnitude for blocks without any cloth is set to zero. Finally, the stretching direction w should be the one in the block whose magnitude is the highest:

$$w = d_k, k = \arg \max_{k \in \{0, 1, \dots, N - 1\}} \{m_k\} \quad (5)$$

B. Select the operation point

The 2D histogram with magnitude of each block in Fig. 3a shows the distribution of the wrinkles on the cloth in Fig. 3b, on which the operation point can therefore be determined based. The algorithm for operation point selection is shown in Alg. 2. In each iteration, we begin with the block containing highest magnitude, indicating the presence of the most wrinkles. The center of this block is denoted by c . Rather than directly targeting the block with the highest magnitude, we select the operation point from among the centers of its eight neighboring blocks to avoid disturbing the wrinkles in the target block. Figure 3a depicts a representation of the center block (c) denoted by a yellow dot and its eight neighboring blocks, referred to as $\{b_i\}$. The red arrow extending from CoM to c is represented by v_{cc} :

$$v_{cc} = c - \text{CoM}$$

Algorithm 1 Calculate stretching direction

Input: block images $\{I_j\}$, center of mass CoM, number of orientations n , number of blocks N
Output: Stretching direction w

```

1: for  $j = 0, 1, \dots, N - 1$  do
2:   for  $i = 0, 1, \dots, n - 1$  do
3:      $\theta_i \leftarrow i \times \pi/n$                                  $\triangleright$  Orientation
4:      $T_i \leftarrow \text{GaborFilter}(I_j, \theta_i)$      $\triangleright$  Intensity map
5:      $l_i \leftarrow \sum t, \forall t \in T_i$   $\triangleright$  Sum up value in each pixel
   in  $T$ 
6:   end for
7:    $m \leftarrow \max \{l_k\}, \forall k \in \{0, 1, \dots, n - 1\}$ 
8:    $d \leftarrow n(\theta_k), k = \arg \max \{l_k\}$      $\triangleright$   $n$ : unit vector
      perpendicular to the  $k^{th}$  orientation
9:   if  $v_{cc} \cdot d \geq 0$  then
10:     $d \leftarrow d$ 
11:   else
12:     $d \leftarrow -d$ 
13:   end if       $\triangleright$  Make  $d$  point outwards the center
14: end for
15:  $w \leftarrow d_k, k = \arg \max \{m_k\}$ 
16: return  $w$ 

```

We use the symbol v_{cb} to denote any of the purple arrows pointing from c to one of its neighboring block center b_i :

$$v_{cb} = c - b_i$$

In order to select an appropriate operation point among the blocks away from CoM relative to c , we evaluate the dot product of v_{cc} and each vector v_{cb} in turn. If the dot product is not positive, the associated block is excluded from further consideration. The operation point is then randomly selected from the remaining candidates by function RandomSelect in Line 8 of Alg. 2. As shown in Fig. 3b, the operation point has been determined through the proposed selection process. It is worth noting that this approach helps to prevent direct contact between the end-effector and the wrinkle during operation. Such contact has the potential to exacerbate the wrinkling, and the selected operation point effectively mitigates this issue.

In summary, our algorithm has following outputs:

- 1) Stretching direction $w \in \mathbb{R}^2$. It is a 2-dimensional vector indicating a proper stretching direction to remove wrinkles.
- 2) Operation point $p(x, y)$. The algorithm determines a point in the image where the end-effector should move, i.e. the pixel coordinate will be given.

IV. EXPERIMENTS

In order to evaluate our proposed method, we conducted a series of experiments in both simulated and real-world scenarios. Specifically, we first validated our approach on wrinkled cloth within the SoftGym simulation environment [28]. Additionally, we conducted experiments using a Franka Emika Robot.

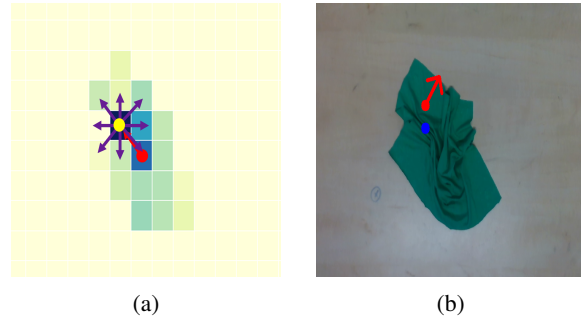


Fig. 3: The heatmap (left) and the corresponding cloth (right). (a) Illustration of center block c (yellow dot), its neighboring blocks $\{b_i\}$, vector v_{cc} (red arrow) and v_{cb} (purple arrows). (b) The center of block with highest magnitude (blue) and the selected operation point (red).

Algorithm 2 Determine the operation point

Input: CoM, c , $\{b_i\}$
Output: operation point p

```

1: for  $b_i$  in  $\{b_i\}$  do
2:    $v_{cc} \leftarrow c - \text{CoM}$ 
3:    $v_{cb} \leftarrow c - b_i$ 
4:   if  $v_{cc} \cdot v_{cb} \geq 0$  then
5:     Insert  $b_i$  into  $P$ 
6:   end if
7: end for
8:  $p \leftarrow \text{RandomSelect}(P)$ 
9: return  $p$ 
```

A. Simulation environment

To facilitate the development and refinement of our proposed algorithms, we employed Softgym [28], a cutting-edge particle-based simulator for non-rigid objects. Through this simulation, we were able to rapidly prototype and fine-tune the hyperparameters of the Gabor filter. The observation generated by the simulation consists of an RGB image with dimensions of 720×720 captured from a top-down perspective. As depicted in the left panel of Figure 4, the directions are perpendicular to the wrinkles in the blocks, which aligns with the expected outcome of our algorithm. Furthermore, the right panel of the figure displays a heatmap that highlights blocks with higher wrinkle density, which corresponds with the distribution of wrinkles shown in the left panel.

B. Real Robot Experiment

To better make use of the direction and operation point in the cloth manipulation task, we have designed and 3D-printed a specialized end-effector. Figure 5 depicts the end-effector mounted on the manipulator. The end-effector has a finger-like shape, which is a combination of a cylinder and a ball. During the manipulation, the ball part comes into contact with the cloth. On the other side of the end-effector, there is a flange connected to the robot. It is worth noting

that this end-effector also restricts the manipulation to a 2D surface.

We evaluate our proposed method on a Franka Emika Robot. In order to obtain RGB image of the cloth on the table from a top-down perspective as input, we mounted an Intel RealSense D435 camera onto the end-effector. For extrinsic calibration, we used OpenCV's chessboard [29] and the Visual Servoing Platform (ViSP) [30] to determine the transformation from pixel coordinates to real-world coordinates. In general, the workflow of the experiment is:

- 1) Place the cloth in the middle of the camera's field of view and manually flatten it before starting the experiment.
- 2) Capture the image of cloth when it is fully flatten and calculate the full coverage.
- 3) Manually make some wrinkles on the cloth.
- 4) The algorithm estimates the coverage and computes the stretching direction and operation point.
- 5) The robot manipulator touches the operation point with its end-effector and drags a fixed distance along the stretching direction.
- 6) The robot moves back up to the starting position to capture a global image, completing one step of the task.
- 7) Repeat Step 4-6 until the coverage meets the stopping criterion.

Note that the coverage in the workflow is computed by dividing the number of pixels in the cloth by the total number of pixels in the image.

Baseline. We conducted a comparative analysis of the performance of our algorithm against three other baseline methods, namely Random, Heuristic, and Human. The Random method randomly selects an operation point within the cloth, while the Heuristic method selects the operation point from candidate points obtained by applying a corner detection algorithm on the cloth. For both Random and Heuristic methods, the stretching direction is determined by the unit vector pointing from CoM to the operation point. On the other hand, the Human method involves a human operator who manually selects the operation point and stretching direction. During this task, the participant observes the cloth from the image captured by the camera and determines the

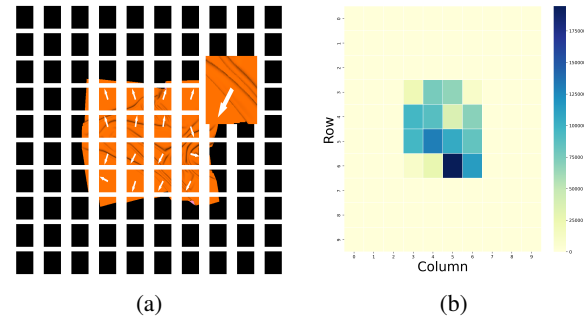


Fig. 4: The direction and heatmap within the simulation environment.

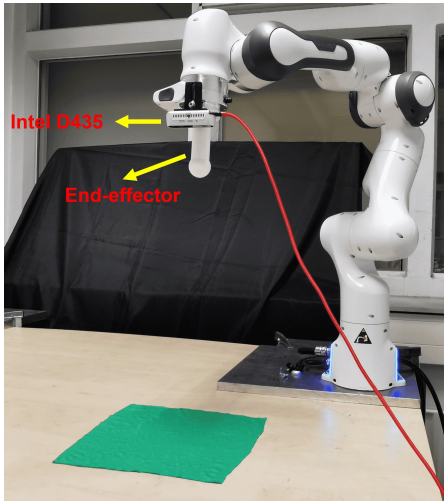


Fig. 5: The robot setup for real experiments.

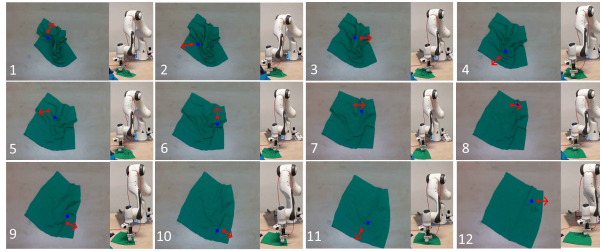


Fig. 6: Cloth flattening by a Franka Emika Robot shown in Fig. 5 when using Proposed method.

manipulation policy by clicking on the window displayed on the screen. The position of the first click corresponds to the operation point, while the stretching direction is determined by a unit vector pointing from the first click to the second click. We collected experimental data from three human operators. Fig. 6 shows a continuous sequence of the robot performing the operation using Proposed method. Table I summarizes how each method determines the manipulation policy.

Evaluation metric. We define two types of coverage when performing the flattening task. The first type is the initial coverage, which is recorded after generating some wrinkles for the first time. The second type is the relative coverage, which is defined as the ratio of the final coverage (F) to the coverage when the cloth is fully flattened (C):

$$R = \frac{F}{C}$$

We set the stopping criterion as achieving a relative coverage greater than 99%. Throughout the task, the relative coverage

TABLE I: Manipulation policy of baseline methods

Name	Operation Point (OP)	Direction
Random	Random point within the cloth	From CoM to OP
Heuristic	Random point around edges	From CoM to OP
Human	Selected by operator	Determined by operator

TABLE II: Number of tasks and steps for different methods used in the experiment. Note that the Proposed method is our algorithm.

Method	Number of tasks		Average number of steps	
	Easy	Hard	Easy	Hard
Random	4	11	7.00	9.36
Heuristic	5	10	5.80	9.50
Proposed	3	12	7.00	8.75
Human	4	11	4.50	6.45

is calculated at each step. Additionally, we measure the number of steps required to meet the stopping criterion as another metric.

V. RESULTS

The initial coverage of all tasks are clustered using k-means [31] into two types. This clustering method enables us to categorize the tasks as either "Easy" or "Hard" based on their initial coverage. We consider the cluster with a higher initial coverage as "Easy", while the cluster with a lower initial coverage is considered "Hard". Table II displays the number of easy and hard tasks for different methods, as well as the average number of steps required to complete these two types of tasks. It is worth noting that every participant performs 5 tasks for each method.

Table II shows that the difficulty distribution of the tasks is approximately in the ratio of easy:hard=1:2. Given a similar proportion of easy and hard tasks, comparing the average number of steps required to complete the tasks is a fair way to evaluate the efficiency of each method. Overall, the Human method outperforms all other methods for both easy and hard tasks, completing tasks in 4.50 and 6.45 steps, respectively.

For easy tasks, the Heuristic method performs better than the Random and Proposed methods, requiring only 5.80 steps compared to 7.00 steps for the other two methods. However, for hard tasks, the Heuristic and Random methods require more steps than the Proposed method to complete the task.

Fig. 7 presents a histogram of the number of steps required by each method to complete the tasks. It shows the frequency of occurrence of different number of steps. The Human method requires at most 9 steps to finish a task, while the Random and Heuristic methods generally need more steps than our Proposed method. Although Random and Heuristic methods may complete a task in fewer steps in some cases, on average, our method requires fewer steps than these baselines and only slightly more steps than the Human method.

VI. CONCLUSIONS AND FUTURE WORK

In this paper, we proposed a promising image-processing algorithm for cloth flattening tasks that successfully infers the wrinkle distribution on the cloth and extracts a low-dimensional representation of the wrinkles. The extracted features are then used to derive a control strategy, including

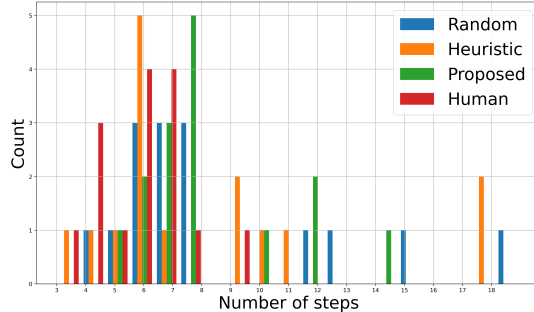


Fig. 7: The frequency of steps for different methods.

a stretching direction and a corresponding operation point, for robot execution. We validated the image-processing algorithm in a simulation environment, SoftGym, and showed that our framework outperforms two other baseline methods for wrinkle removal of crumpled cloth on a table in a real robot experiment. Although the proposed method did not exceed the performance of human operators, our results demonstrate the promise of our approach for addressing this task.

In the future, we plan to incorporate learning-based methods into our framework to improve its performance. While our current algorithm outperforms two baseline methods, it still falls short of human operators' decision-making abilities. Therefore, we plan to explore Learning from Demonstration (LfD) methods to close this performance gap and enhance the quality of the control strategy generated by the algorithm. Additionally, we aim to integrate our method with other cloth representation techniques to create a more robust and adaptive framework capable of handling a wider range of DOM tasks.

REFERENCES

- [1] H. Yin, A. Varava, and D. Kragic, "Modeling, learning, perception, and control methods for deformable object manipulation," *Science Robotics*, vol. 6, no. 54, p. eabd8803, 2021.
- [2] J. Zhu, A. Cherubini, C. Dune, D. Navarro-Alarcon, F. Alambeigi, D. Berenson, F. Ficuciello, K. Harada, J. Kober, X. Li *et al.*, "Challenges and outlook in robotic manipulation of deformable objects," *IEEE Robotics & Automation Magazine*, vol. 29, no. 3, pp. 67–77, 2022.
- [3] L. Sun, G. A. Camarasa, A. Khan, S. Rogers, and P. Siebert, "A precise method for cloth configuration parsing applied to single-arm flattening," *International Journal of Advanced Robotic Systems*, vol. 13, no. 2, p. 70, mar 2016.
- [4] C. Bersch, B. Pitzer, and S. Kammel, "Bimanual robotic cloth manipulation for laundry folding," in *2011 IEEE/RSJ International Conference on Intelligent Robots and Systems*. IEEE, sep 2011, pp. 1413–1419.
- [5] S. Miller, J. van den Berg, M. Fritz, T. Darrell, K. Goldberg, and P. Abbeel, "A geometric approach to robotic laundry folding," *The International Journal of Robotics Research*, vol. 31, no. 2, pp. 249–267, dec 2011.
- [6] J. Stria, D. Prusa, V. Hlavac, L. Wagner, V. Petrik, P. Krsek, and V. Smutny, "Garment perception and its folding using a dual-arm robot," in *2014 IEEE/RSJ International Conference on Intelligent Robots and Systems*. IEEE, sep 2014, pp. 61–67.
- [7] X. Ma, D. Hsu, and W. S. Lee, "Learning latent graph dynamics for visual manipulation of deformable objects," 2021.
- [8] M. Saveriano, F. J. Abu-Dakka, A. Kramberger, and L. Peternel, "Dynamic movement primitives in robotics: A tutorial survey," 2021.
- [9] C. E. Rasmussen, "Gaussian processes in machine learning," in *Advanced Lectures on Machine Learning*. Springer Berlin Heidelberg, 2004, pp. 63–71.
- [10] Y. Wu, W. Yan, T. Kurutach, L. Pinto, and P. Abbeel, "Learning to manipulate deformable objects without demonstrations," 2019.
- [11] R. Jangir, G. Alenya, and C. Torras, "Dynamic cloth manipulation with deep reinforcement learning," 2019.
- [12] Y. Tsurumine, Y. Cui, E. Uchibe, and T. Matsubara, "Deep reinforcement learning with smooth policy update: Application to robotic cloth manipulation," *Robotics and Autonomous Systems*, vol. 112, pp. 72–83, feb 2019.
- [13] A. Ramisa, G. Alenya, F. Moreno-Noguer, and C. Torras, "Using depth and appearance features for informed robot grasping of highly wrinkled clothes," in *2012 IEEE International Conference on Robotics and Automation*. IEEE, may 2012.
- [14] A. Caporali and G. Palli, "Pointcloud-based identification of optimal grasping poses for cloth-like deformable objects," in *2020 25th IEEE International Conference on Emerging Technologies and Factory Automation (ETFA)*. IEEE, sep 2020, pp. 581–586.
- [15] T. S. Lee, "Image representation using 2d gabor wavelets," *IEEE Transactions on Pattern Analysis and Machine Intelligence*, vol. 18, no. 10, pp. 959–971, 1996.
- [16] K. Yamazaki and M. Inaba, "A cloth detection method based on image wrinkle feature for daily assistive robots," in *MVA*, 2009, pp. 366–369.
- [17] B. Jia, Z. Hu, J. Pan, and D. Manocha, "Manipulating highly deformable materials using a visual feedback dictionary," 2017.
- [18] B. Jia, Z. Pan, Z. Hu, J. Pan, and D. Manocha, "Cloth manipulation using random-forest-based imitation learning," 2018.
- [19] W. Yan, A. Vangipuram, P. Abbeel, and L. Pinto, "Learning predictive representations for deformable objects using contrastive estimation," 2020.
- [20] P. Chang and T. Padir, "Model-based manipulation of linear flexible objects: Task automation in simulation and real world," *Machines*, vol. 8, no. 3, p. 46, aug 2020.
- [21] R. Hoque, D. Seita, A. Balakrishna, A. Ganapathi, A. K. Tanwani, N. Jamali, K. Yamane, S. Iba, and K. Goldberg, "Visuospatial foresight for multi-step, multi-task fabric manipulation," 2020.
- [22] J. Matas, S. James, and A. J. Davison, "Sim-to-real reinforcement learning for deformable object manipulation," 2018.
- [23] A. Singh, L. Yang, K. Hartikainen, C. Finn, and S. Levine, "End-to-end robotic reinforcement learning without reward engineering," 2019.
- [24] B. Zhang and P. Liu, "Model-based and model-free robot control: A review," in *Lecture Notes in Mechanical Engineering*. Springer Singapore, 2021, pp. 45–55.
- [25] A. Pinosky, I. Abraham, A. Broad, B. Argall, and T. D. Murphrey, "Hybrid control for combining model-based and model-free reinforcement learning," *The International Journal of Robotics Research*, p. 027836492210833, jun 2022.
- [26] R. P. Joshi, N. Koganti, and T. Shibata, "Robotic cloth manipulation for clothing assistance task using dynamic movement primitives," in *Proceedings of the Advances in Robotics on - AIR '17*. ACM Press, 2017.
- [27] G. Salhotra, I.-C. A. Liu, M. Dominguez-Kuhne, and G. S. Sukhatme, "Learning deformable object manipulation from expert demonstrations," *IEEE Robotics and Automation Letters*, 2022.
- [28] X. Lin, Y. Wang, J. Olkin, and D. Held, "Softgym: Benchmarking deep reinforcement learning for deformable object manipulation," 2020.
- [29] G. Bradski, "The OpenCV Library," *Dr. Dobb's Journal of Software Tools*, 2000.
- [30] E. Marchand, F. Spindler, and F. Chaumette, "Visp for visual servoing: a generic software platform with a wide class of robot control skills," *IEEE Robotics and Automation Magazine*, vol. 12, no. 4, pp. 40–52, December 2005.
- [31] S. Lloyd, "Least squares quantization in pcm," *IEEE Transactions on Information Theory*, vol. 28, no. 2, pp. 129–137, 1982.